International Journal of Development Mathematics Vol 2 Issue 1 Page No. 001 - 021

INTERNATIONAL JOURNAL OF DEVELOPMENT MATHEMATICS

ISSN: 3026-8656 (Print) | 3026-8699 (Online)

journal homepage: https://ijdm.org.ng/index.php/Journals

Attainable Order of Hybrid Methods from Polynomial Nodes for Non-Linear Singularly Perturbed Initial Value Problems

Dauda G. Yakubu[a*], Isah Abdullahi[a], Ali Musa[b], Abdullahi M. Gamsha[a]

[a]Department of Mathematical Sciences, Abubakar Tafawa Balewa University, Bauchi, Nigeria

[b]Department of Mathematics and Statistics, Yobe State University, Damaturu, Nigeria

A R T I C L E   I N F O

Article history:
Received 20 February 2025
Received in revised form 20 March 2025
Accepted 28 Marchr 2025

Keywords:
Hybrid method, Continuous scheme,
Singularly perturbed initial value problem,
Stiff oscillatory system

MSC 2020 Subject classification:
34A30, 34A34, 92B05, 92-10

A B S T R A C T

We develop hybrid methods utilizing collocation at polynomial nodes for the numerical integration of singularly perturbed non-linear initial-value problems. The present methods are intended for solving nonlinear singularly perturbed initial value problems without linearization and provide third and fourth-order convergence results. We use piecewise-uniform meshes which resolve the difficulties arising from the steep gradient of the solution in the initial layer. Linear stability of these methods are studied. Numerical experiments are carried out to verify the efficiency and accuracy of the methods. The new hybrid integrators are effectively employed to achieve accurate representation of singularly perturbed systems, providing physical interpretation of what they represent in natural phenomena. These are illustrated through phase plots that exhibit unusual and novel behaviors. The resulting surface phase plot curves represent portions of the phase space of a perturbed system, frequently illustrating real world observed phenomena. These are depicted graphically as surface phase plot curves shown in Figures, while numerical values are presented side by side in Tables.

1. Introduction

Singular perturbation problems occur in numerous applied fields, including fluid dynamics, optimal control, chemical reactor theory, dynamics of dry-flowing avalanches, etc. We shall be interested in the singular perturbation problem obtained as the small positive parameter ε tends to zero. Singularly perturbed system of ordinary differential equation can be written in the form,

$$\begin{cases} \varepsilon y' = f(x, y(x)), & 0 \le x \le 1, \\ y(x_0) = y_0, & \end{cases} \tag{1}$$

on a bounded interval (say, $0 \le x \le 1$) with smooth vector function f of dimensions m and with prescribed initial vectors $y(x_0)$. There are challenges in numerically integrating (1) because the solution frequently exhibits a narrow initial boundary layer region of rapid change and so-called stiffness in the outer region where $x > 0$. The equation develops insight and intuition based on a sequence of solvable model problems, and it relates a variety of literature scattered throughout asymptotic and numerical analyses, stability and control theory and some specific topics in applied mathematical modeling. The existence of a small parameter ε in particular which is associated with the highest derivative leads to the inadequacy of traditional numerical methods in producing satisfactory results.

Consequently, it is essential to explore specialized techniques for the numerical resolution of singular perturbation problem of the type in equation (1). It fosters understanding and intuition through a series of manageable model problems, while also connecting diverse literature found across asymptotic and numerical analyses, stability and control theory, as well as some subjects in applied mathematical modeling. Our focus will be

* Corresponding author. Tel.: +2348052168433
E-mail address: daudagyakubu@gmail.com (Dauda G. Yakubu)
https://doi.org/10.62054/ijdm/0201.01

on the singular perturbation problem that arises as the small positive parameter ε approaches zero. Experimental and theoretical findings indicate that an adiabatic tubular reactor, undergoing a straightforward first-order irreversible exothermic chemical reaction, may display multiple stable steady states. The chemical and mathematical frameworks for these phenomena are detailed in the works of Aris (1969) and Ramos et al. (2010). The mathematical representations of these chemical reactions consist of differential equations where the highest order derivative is multiplied by a small positive parameter ε as shown in equation (1). Specifically, one should examine the nonlinear initial value problem that emerges in the context of chemical reactions as given in Burghardt and Zaleski (1968). Some challenging illustrative examples are considered in detail.

Definition 1.1: Butcher (2003). *The function f satisfies a one-sided Lipschitz condition, with one-sided Lipschitz constant l, if for all $x \in [a, b]$ and all $u, v \in R^N$,*

$$\langle f(x,u) - f(x,v), u - v \rangle \le l\|u - v\|^2,$$

where the norm is defined by $\|u\|^2 = \langle u, u \rangle$ assuming that there exists an inner product on R^N.

It is possible that a problem will have a very large Lipschitz constant, but a manageable one-sided Lipschitz constant. This can help us find realistic growth estimates for the effects of perturbations, as can be seen in the following theorem.

Theorem 1.1: Butcher (1987), *If f satisfies a one-sided Lipschitz condition with constant l, and y and z are each solutions of (1) then for all $x \ge x_0$,*

$$\|y(x) - z(x)\| \le \exp(l(x - x_0))\|y(x_0) - z(x_0)\|.$$

From this result, it shows that the distance between any two solutions will not increase rapidly or may even decrease if the equation has an adequate one-sided Lipschitz constant. Since stiffness is closely related to the behavior of perturbations to a given solution, it is important to find out the effect of small perturbations with a one-sided Lipschitz condition.

Consider the type of equation in (1) with $y(x)$, a solution, and $\varepsilon Y(x)$, a small perturbation to the given solution. Replace $y(x)$ in the equation by $y(x) + \varepsilon Y(x)$ and expand the solution in a series in powers of ε up to the second order, then we get,

$$y'(x) + \varepsilon Y'(x) = f(x, y(x)) + \varepsilon \frac{\partial f}{\partial y} Y(x). \tag{2a}$$

Subtract the equation in (1) from equation (2a) and simplify it, then finally obtain the equation which controls the behavior of the perturbation,

$$\begin{aligned} Y'(x) &= \frac{\partial f}{\partial y} Y(x) \\ &= J(x)Y(x), \end{aligned} \tag{2b}$$

where $J(x)$ is the Jacobian matrix of $f(x, y(x))$. We can use the spectrum of eigen-values of $J(x)$ to characterize stiffness. The eigen-values of $J(x)$ determine the growth rate of the perturbation with a moderate change in the value of the solution and a very small change in $J(x)$ in a time interval Δx. The existence of one or more large and negative values of λ where $\lambda \in \sigma(J(x))$ and $x \in \Delta x$ indicates that the stiffness is present.

To find the approximate solution of (1) based on Taylor series method of expansion we consider a polynomial of the form in Yakubu et al. (2017) given by

$$y(x) = \alpha_0 + \alpha_1 x + \alpha_2 x^2 + \cdots + \alpha_{p-1} x^{p-1} = \sum_{i=0}^{p-i} \alpha_i x^i \, . \tag{2c}$$

Setting $p = t + s$ to be able to determine uniquely $\{\alpha_i\}$ where $t > 0$ stands for the interpolation points used and $s > 0$ are the distinct collocation points chosen from the interval $\bar{x}_j \in \{x_n, x_{n+1}\}$. Our main objective is to utilize not only the interpolation points $\{x_{n+i}\}$ but also several collocation points on the interpolation interval by differentiating equation (2c) to fit both $y(x)$ and $y'(x)$ in the sense of Yakubu et al. (2017). To determine the parameters $\{\alpha_i\}, i = 0,1,2,\ldots, p-1$, we consider the following interpolation and collocation conditions as follows:

$$\begin{cases} y_{n+i} = y(x_n + ih), & i \in \{0,1,2,\ldots,t-1\}, \\ y'_{n+j} = f_{n+j} = f(x_n + jh, y(x_n + jh)), & (j = 0,1,2,\ldots,s-1). \end{cases} \tag{3}$$

When we combine the expression in (2c) with the interpolation and collocation conditions in (3), we obtain a matrix form of equation as follows:

$$DC = I \, , \tag{4}$$

where I is an identity matrix of appropriate dimension

$$C = \begin{pmatrix} \vartheta_{1,0} & \cdots & \vartheta_{1,t-1} & h\upsilon_{1,0} & \cdots & h\upsilon_{1,s-1} \\ \vartheta_{2,0} & \cdots & \vartheta_{2,t-1} & h\upsilon_{2,0} & \cdots & h\upsilon_{2,s-1} \\ \vartheta_{3,0} & \cdots & \vartheta_{3,t-1} & h\upsilon_{3,0} & \cdots & h\upsilon_{3,s-1} \\ \vartheta_{4,0} & \cdots & \vartheta_{4,t-1} & h\upsilon_{4,0} & \cdots & h\upsilon_{4,s-1} \\ \vdots & \ddots & \vdots & \vdots & \ddots & \vdots \\ \vartheta_{p-1,0} & \cdots & \vartheta_{p-1,t-1} & h\upsilon_{p-1,0} & \cdots & h\upsilon_{p-1,s-1} \end{pmatrix} = D^{-1} \tag{5}$$

and

$$D = \begin{pmatrix} 1 & x_n & x_n^2 & x_n^3 & \cdots & x_n^{p-1} \\ \vdots & \vdots & \vdots & \vdots & \ddots & \vdots \\ 1 & x_{n+t-1} & x_{n+t-1}^2 & x_{n+t-1}^3 & \cdots & x_{n+t-1}^{p-1} \\ 0 & 1 & 2x_n & 3x_n^2 & \cdots & D'x_n^{p-2} \\ \vdots & \vdots & \vdots & \vdots & \ddots & \vdots \\ 0 & 1 & 2x_{n+s-1} & 3x_{n+s-1}^2 & \cdots & D'x_{n+s-1}^{p-2} \end{pmatrix} \tag{6}$$

where D' in (6) represent the first derivative corresponding to the differentiation with respect to x. Similar to the Vander Monde matrix, D in equation (4) is non-singular. Therefore, a close form solution for the system in equation (4) is presented which has been obtained by considering the inverse of D, that is,

$$C = D^{-1}. \tag{7}$$

Re-arranging equations (4)-(7) to have the multistep collocation formula of the form

$$y(x) = \sum_{j=0}^{t-1} \vartheta_j(x) y_{n+j} + h \sum_{j=0}^{s-1} \upsilon_j(x) f_{n+j}\ , \tag{8}$$

where $\vartheta_j(x)$ and $\upsilon_j(x)$ are continuous coefficients of the method and are assumed polynomials of the form

$$\vartheta_j(x) = \sum_{i=0}^{t+s-1} \vartheta_{j,i+1} x^i, \qquad j \in \{0,1,2,\ldots,t-1\}, \tag{9}$$

$$h\upsilon_j(x) = h \sum_{i=0}^{t+s-1} \upsilon_{j,i+1} x^i, \quad j = 0,1,2,\ldots s-1. \tag{10}$$

The step size h in equation (8) can be a constant or varied in the numerical integration process. The basis function $\{x^i\}$ in equations (9) and (10) is defined by

$$W_i(x) = \sum_{i=0}^{p-1} x^i \ .$$

Here y and f are smooth real N-dimension vector functions. The numerical constants coefficients $\vartheta_{j,i+1}$ and $\upsilon_{j,i+1}$ in equations (9) and (10) are to be determined. In fact, the above constants coefficients can be obtained from the component of the matrix D^{-1}. The choice $C = D^{-1}$ leads to the determination of the numerical constants $\vartheta_{j,i+1}$ and $\upsilon_{j,i+1}$ in equations (9) and (10) respectively. Actual evaluation of the matrices D and C are carried out with a computer algebra system, for example maple software.

2. The Solution Methods

2.1 Hybrid method from polynomial nodes of order 3 with two off-step points

In this section we consider some hybrid methods which will be competitive with their counterparts in literature by careful selection of the collocation points, which will make the methods to have smaller error constants and zero-stable. This is because among the hybrid methods, those with smaller error constants, *A*-stable and *L*-stable are preferred when integrating differential equations. Therefore, the $(M-1)$ collocation points called the intra-step points are introduced to improve the accuracy of the methods. They are denoted by u , v and specifically chosen to ensure that the methods can accurately integrate linear and nonlinear singularly perturbed initial value problems and to maintain the zero-stability (see, Fatunla (1991). Following Yakubu et al.(2017) we obtain the first hybrid method and the coefficients are compactly shown below,

$$\begin{bmatrix} y_{n+u} \\ y_{n+v} \\ y_{n+1} \end{bmatrix} = \begin{bmatrix} y_n \\ y_n \\ y_n \end{bmatrix} + h \begin{bmatrix} \frac{-205+65\sqrt{5} y'_n}{120} \\ \frac{-205-65\sqrt{5} y'_n}{120} \\ \frac{5 y'_n}{60} \end{bmatrix} + h \begin{bmatrix} \frac{-35+19\sqrt{5}}{120} & \frac{205-89\sqrt{5}}{120} & \frac{95-55\sqrt{5}}{120} \\ \frac{205+89\sqrt{5}}{120} & \frac{-35-19\sqrt{5}}{120} & \frac{95+55\sqrt{5}}{120} \\ \frac{25+12\sqrt{5}}{60} & \frac{25-12\sqrt{5}}{60} & \frac{5}{60} \end{bmatrix} \begin{bmatrix} y'_{n+u} \\ y'_{n+v} \\ y'_{n+1} \end{bmatrix} \tag{11}$$

.

2.2 Hybrid method from polynomial nodes of order 4 with three off-step points

The second method, here we choose the collocation points very carefully to have a better and accurate method of higher order with requirements as specified above in the first subsection. Therefore, in addition to the interior collocation points u and v we select w to have three accurate interior collocation points, as shown below:

$$\begin{bmatrix} y_{n+u} \\ y_{n+w} \\ y_{n+v} \\ y_{n+1} \end{bmatrix} = \begin{bmatrix} y_n \\ y_n \\ y_n \\ y_n \end{bmatrix} + h \begin{bmatrix} \frac{-21270+9150\sqrt{5}y_n'}{3600} \\ \frac{5530y_n'}{9600} \\ \frac{-21270-9150\sqrt{5}y_n'}{3600} \\ \frac{1140y_n'}{3600} \end{bmatrix} + h \begin{bmatrix} \frac{1974-870\sqrt{5}}{3600} & \frac{24192-11520\sqrt{5}}{3600} & \frac{9174-4110\sqrt{5}}{3600} & \frac{-12270+5550\sqrt{5}}{3600} \\ \frac{464+270\sqrt{5}}{9600} & -\frac{2688}{9600} & \frac{464-270\sqrt{5}}{9600} & \frac{1030}{9600} \\ \frac{9174+4110\sqrt{5}}{3600} & \frac{24192+11520\sqrt{5}}{3600} & \frac{1974+870\sqrt{5}}{3600} & \frac{-12270-5550\sqrt{5}}{3600} \\ \frac{1788+720\sqrt{5}}{3600} & \frac{2304}{3600} & \frac{1788-720\sqrt{5}}{3600} & \frac{-1440}{3600} \end{bmatrix} \begin{bmatrix} y'_{n+u} \\ y'_{n+w} \\ y'_{n+v} \\ y'_{n+1} \end{bmatrix} \quad (12)$$

The application of the derived methods is very easy, since it should be in block solution form.

3.0 Analysis of the numerical properties of the hybrid methods

3.1 Order of the hybrid methods

Order of a method is one of the fundamental properties of a new derived method, aside zero-stability and consistency, order of convergence and stability characteristics. Therefore, here we calculate the order of the derived methods. We demonstrate the calculation of order using method (12) in subsection 2.2 above, following Lambert (1973) page 23, we have

$$\vartheta_0 = -\begin{bmatrix} 1 \\ 1 \\ 1 \\ 1 \end{bmatrix}, \quad \vartheta_u = \begin{bmatrix} 1 \\ 0 \\ 0 \\ 0 \end{bmatrix}, \quad \vartheta_w = \begin{bmatrix} 0 \\ 1 \\ 0 \\ 0 \end{bmatrix}, \quad \vartheta_v = \begin{bmatrix} 0 \\ 0 \\ 1 \\ 0 \end{bmatrix}, \quad \vartheta_1 = \begin{bmatrix} 0 \\ 0 \\ 0 \\ 1 \end{bmatrix},$$

$$\upsilon_0 = \begin{bmatrix} \frac{-21270+9150\sqrt{5}}{3600} \\ \frac{5530}{9600} \\ \frac{-21270-9150\sqrt{5}}{3600} \\ \frac{-1140}{3600} \end{bmatrix}, \quad \upsilon_u = \begin{bmatrix} \frac{1974-870\sqrt{5}}{3600} \\ \frac{464+270\sqrt{5}}{9600} \\ \frac{9174+4110\sqrt{5}}{3600} \\ \frac{1788+720\sqrt{5}}{3600} \end{bmatrix}, \quad \upsilon_w = \begin{bmatrix} \frac{24192-11520\sqrt{5}}{3600} \\ \frac{-2688}{9600} \\ \frac{24192+11520\sqrt{5}}{3600} \\ \frac{2304}{3600} \end{bmatrix},$$

$$\upsilon_v = \begin{bmatrix} \frac{9174-4110\sqrt{5}}{3600} \\ \frac{464-270\sqrt{5}}{9600} \\ \frac{1974+870\sqrt{5}}{3600} \\ \frac{1788-720\sqrt{5}}{3600} \end{bmatrix}, \quad \upsilon_1 = \begin{bmatrix} \frac{-2270+5550\sqrt{5}}{3600} \\ \frac{1030}{9600} \\ \frac{-12270-5550\sqrt{5}}{3600} \\ \frac{-14407}{3600} \end{bmatrix}.$$

To obtain the order, we substitute the above matrices into the following, to have

$$C_0 = \vartheta_0 + \vartheta_u + \vartheta_w + \vartheta_v + \vartheta_1 = 0$$

$$C_1 = \left[\vartheta_1 + (u)\vartheta_u + (w)\vartheta_w + (v)\vartheta_v\right] - \left(\upsilon_0 + \upsilon_u + \upsilon_w + \upsilon_v + \upsilon_1\right) = 0$$

$$C_2 = \tfrac{1}{2!}\left[\vartheta_1 + (u)^2\vartheta_u + (w)^2\vartheta_w + (v)^2\vartheta_v\right] - \left(\upsilon_1 + (u)\upsilon_u + (w)\upsilon_w + (v)\upsilon_v\right) = 0$$

$$C_3 = \tfrac{1}{3!}\left[\vartheta_1 + (u)^3\vartheta_u + (w)^3\vartheta_w + (v)^3\vartheta_v\right] - \left(\tfrac{1}{2}\right)\left[\upsilon_1 + (u)^2\upsilon_u + (w)^2\upsilon_w + (v)^2\upsilon_v\right] = 0$$

$$C_4 = \tfrac{1}{4!}\left[\vartheta_1 + (u)^4\vartheta_u + (w)^4\vartheta_w + (v)^4\vartheta_v\right] - \left(\tfrac{1}{3!}\right)\left[\upsilon_1 + (u)^3\upsilon_u + (w)^3\upsilon_w + (v)^3\upsilon_v\right] = 0$$

$$C_5 = \tfrac{1}{5!}\left[\vartheta_1 + (u)^5\vartheta_u + (w)^5\vartheta_w + (v)^5\vartheta_v\right] - \left(\tfrac{1}{4!}\right)\left[\upsilon_1 + (u)^4\upsilon_u + (w)^4\upsilon_w + (v)^4\upsilon_v\right] \neq 0$$

and after routine algebraic simplifications we have

$$C_0 = C_1 = C_2 = C_3 = C_4 = 0, \textbf{ but } C_5 \neq 0.$$

This shows that the highest order of the newly derived hybrid methods have attainable order of four (4) with error constants displayed in Table 1.

3.2 Zero-stability analysis of the hybrid methods

If a numerical method for singularly perturbed or singly perturbed or dynamical systems of ordinary differential equations advances the solution in time while maintaining the stability of the trivial solution, that is, the solution in which all variables equal zero, it is referred to as zero-stable. This implies that any little changes to the initial circumstances won't grow or make the solution limitless; rather, they will stay modest as the solution is calculated. For numerical methods, zero stability is a crucial feature since it guarantees that the method will yield significant findings even in cases when the initial conditions are only roughly known. Zero-stability assessments, which involve applying the method to test issues and analyzing the behavior of the solution, can be used to evaluate the stability of numerical methods. As the solution is calculated, a numerical method that is not zero-stable may yield solutions that deviate from the actual solution or become unbounded. In these situations, the method can be deemed untrustworthy and might require revision or improvement to yield more accurate findings. By effectively considering a numerical approach as a difference scheme, zero-stability offers a way to analyze its stability. Well-posedness of the resulting difference scheme is equivalent to zero-stability of a numerical method. Therefore to determine the zero-stability of the hybrid methods the following equations results from writing the hybrid method in matrix form:

$$U^{(1)}Y_\mu = U^{(0)}Y_{\mu-1} + h\left(V^{(0)}F_{\mu-1} + V^{(1)}F_\mu\right), \tag{13}$$

where

$$Y_\mu = \left(y_{n+u}, y_{n+w}, y_{n+v}, y_{n+1}\right)^T, \; Y_{\mu-1} = \left(y_{n-u}, y_{n-w}, y_{n-v}, y_n\right)^T,$$

$$F_\mu = \left(f_{n+u}, f_{n+w}, f_{n+v}, f_{n+1}\right)^T, \; F_{\mu-1} = \left(f_{n-u}, f_{n-w}, f_{n-v}, f_n\right)^T,$$

and $U^{(1)}, U^{(0)}, V^{(1)}$ and $V^{(0)}$ in this case are maximum of 4 by 4 matrices with their corresponding entries given by the coefficients of the methods in subsection (2.2). The matrices for the method are given as below where $U^{(1)}$ is the matrix identity and of dimension 4,

$$U^{(1)} = \begin{bmatrix} 1 & 0 & 0 & 0 \\ 0 & 1 & 0 & 0 \\ 0 & 0 & 1 & 0 \\ 0 & 0 & 0 & 1 \end{bmatrix}, \quad U^{(0)} = \begin{bmatrix} 0 & 0 & 0 & 1 \\ 0 & 0 & 0 & 1 \\ 0 & 0 & 0 & 1 \\ 0 & 0 & 0 & 1 \end{bmatrix}, \tag{14}$$

$$V^{(0)} = \begin{bmatrix} \frac{-21270+9150\sqrt{5}}{3600} \\ \frac{5530}{9600} \\ \frac{-21270-9150\sqrt{5}}{3600} \\ \frac{1140}{3600} \end{bmatrix}, \quad V^{(1)} = \begin{bmatrix} \frac{1974-870\sqrt{5}}{3600} & \frac{24192-11520\sqrt{5}}{3600} & \frac{9174-4110\sqrt{5}}{3600} & \frac{-12270+5550\sqrt{5}}{3600} \\ \frac{464+270\sqrt{5}}{9600} & -\frac{2688}{9600} & \frac{464-270\sqrt{5}}{9600} & \frac{1030}{9600} \\ \frac{9174+4110\sqrt{5}}{3600} & \frac{24192+11520\sqrt{5}}{3600} & \frac{1974+870\sqrt{5}}{3600} & \frac{-12270-5550\sqrt{5}}{3600} \\ \frac{1788+720\sqrt{5}}{3600} & \frac{2304}{3600} & \frac{1788-720\sqrt{5}}{3600} & \frac{-1440}{3600} \end{bmatrix}.$$

The zero-stability is always the stability of the difference system by taking the limit when h tends to zero. Hence, as $h \to 0$, the method in (12) becomes,

$$U^{(1)}Y_{\mu} - U^{(0)}Y_{\mu-1} = 0, \tag{15}$$

with $\rho(R)$ as the first characteristic polynomial of the system written as

$$\rho(R) = \det\left(RU^{(1)} - U^{(0)}\right). \tag{16}$$

Substituting the matrices $U^{(1)}$ and $U^{(0)}$ from equation (14), into (16) we have

$$\rho(R) = \left(R\begin{bmatrix} 1 & 0 & 0 & 0 \\ 0 & 1 & 0 & 0 \\ 0 & 0 & 1 & 0 \\ 0 & 0 & 0 & 1 \end{bmatrix} - \begin{bmatrix} 0 & 0 & 0 & 1 \\ 0 & 0 & 0 & 1 \\ 0 & 0 & 0 & 1 \\ 0 & 0 & 0 & 1 \end{bmatrix} \right). \tag{17}$$

Simplifying (17) to obtain,

$$\rho(R) = R^3(R-1) = 0, \;\; \Rightarrow R = (0,0,0,1). \tag{18}$$

Since $R = (0,0,0,1)$ the method in (12) is zero stable.

Similarly, it is possible to show that method (11) is zero-stable following the same calculation.

Definition 3.1: Lambert (1973) (Zero-stable) *The family of methods in (8) are said to be zero-stable if the roots condition*

$$\rho(\lambda) = \det\left[\sum_{i=0}^{k} A^i \lambda^{k-1}\right] = 0, \tag{19}$$

satisfies the inequality $|\lambda_j| \le 1, \; j = 1, 2, 3, \ldots, k$. *But when the inequality reduces to* $|\lambda_j| = 1$, *then the multiplicity should not be greater than one.*

Based on definition 3.1, the newly derived hybrid methods are zero-stable which are attractive for handling dynamical systems as well as singularly perturbed initial value problems.

Table 1 displays the derived hybrid collocation methods' orders and error constants based on our computations. The Table makes it evident that the hybrid collocation techniques are higher-order and, therefore, more accurate than some of the current collocation techniques in literature.

Table 1: Order and Error Constants of the Hybrid Collocation Methods

Method	Order	Error constants
Method (11)	**i)** y_{n+1}, **P = 3**	**C4 = 6.4583**$\times 10^{-2}$
	ii) y_{n+u}, **P = 3**	**C4 = 6.3750**$\times 10^{-1}$
	iii) y_{n+v}, **P = 3**	**C4 = 3.3333**$\times 10^{-2}$
Method (12)	**i)** y_{n+u}, **P = 4**	**C5 = 9.8958**$\times 10^{-2}$
	ii) y_{n+w}, **P = 4**	**C5 = 3.1250**$\times 10^{-2}$
	iii) y_{n+v}, **P = 4**	**C5 = 4.6875**$\times 10^{-2}$
	iv) y_{n+1}, **P = 4**	**C5 = 7.4404**$\times 10^{-2}$

Definition 3.2: Lambert (1973) (Consistency) *The family of methods in (8) are consistent if the order p of the method satisfy the inequality* $p \geq 1$,

(i) $\rho(1) = 0$ *and*

(ii) $\rho'(1) = \sigma(1)$, *where* $\rho(z)$ *and* $\sigma(z)$ *are 1st and 2nd characteristic polynomials which are assumed to have no common factor.*

From Table 1 and definition 3.1, we can attest that the derived hybrid collocation methods are consistent.

Definition 3.3: Lambert (1991) (*A(*α*)-stable). The family of methods in (8) are A(*α*)-stable if the inequality* $0 < \alpha \leq \pi / 2$ *and the angular sector*

$$S_\alpha = \{z \in C : |\arg(-z)| < \alpha, z \neq 0\},$$

is contained in the stability domain $\Re$.

When the interval of absolute stability consists of the negative real axis, the method is said to be $A_0 - stable$.

Definition 3.4: Ramos and Patricio (2014) *The family of methods given in (8) are said to be irreducible if the continuous coefficients* $\vartheta_j(x)$ *and* $\upsilon_j(x)$ *have no common factor.*

3.3 Order of convergence of the hybrid numerical integration methods

The order of convergence of the recently derived block hybrid numerical integrators (methods) is examined in this section. We give some definitions to aid in our analysis of the convergence of the techniques. We use the block approach described in (12) as an example.

Definition 3.5: Lambert (1973) *A function* $f(x, y)$ *satisfies the Lipschitz condition on the domain* $D \subseteq \Re^2$ *if there exists a constant* $L > 0$ *such that,*

$$\left| f(x, y) - f(x, y^*) \right| \leq L \left| y - y^* \right|,$$

for all $(x, y), (x, y^*) \in D$.

Definition 3.6: *A linear multistep method (LMM) is said to be convergent, if for all initial value problem subject to the above Lipschitz condition:*

$$\lim_{h \to 0} y_n = y^*(x_n),$$

for all solutions $\{y_n\}$ *of the method (see, Lambert (1973).*

Assuming that the exact solution of y_{n+1} is y^*_{n+1} which is written precisely as

$$y_{n+1}^{*}=y_{n}^{*}-\frac{1140hf_{n}}{3600}+\frac{\left(1788+720\sqrt{5}\right)hf_{n+u}}{3600}+\frac{2304hf_{n+w}}{3600}+\frac{\left(1788-720\sqrt{5}\right)hf_{n+v}}{3600}-\frac{1140hf_{n+1}}{3600}$$
$$+\frac{25}{366}h^{5}y^{*(5)}\left(\xi_{n}\right)+R_{6},$$

where R_6 is the remainder term. Subtract y_{n+1} from y_{n+1}^{*} to obtain

$$y_{n+1}^{*}-y_{n+1}=y_{n}^{*}-y_{n}-\frac{1140h}{3600}\left[f\left(x_{n},y_{n}^{*}\right)-f\left(x_{n},y_{n}\right)\right]+\frac{\left(1788+720\sqrt{5}\right)h}{3600}\left[f\left(x_{n+u},y_{n+u}^{*}\right)-f\left(x_{n+u},y_{n+u}\right)\right]$$
$$+\frac{2304h}{3600}\left[f\left(x_{n+w},y_{n+w}^{*}\right)-f\left(x_{n+w},y_{n+w}\right)\right]+\frac{\left(1788-720\sqrt{5}\right)h}{3600}\left[f\left(x_{n+v},y_{n+v}^{*}\right)-f\left(x_{n+v},y_{n+v}\right)\right]$$
$$-\frac{1140h}{3600}\left[f\left(x_{n+1},y_{n+1}^{*}\right)-f\left(x_{n+1},y_{n+1}\right)\right]+\frac{25h^{5}}{336}y^{*(5)}\left(\xi_{n}\right)+R_{6}.$$

Letting $d_{n}=y_{n}^{*}-y_{n},\ldots,d_{n+v}=y_{n+v}^{*}-y_{n+v}, d_{n+1}=y_{n+1}^{*}-y_{n+1}$, then we have

$$\left|d_{n+1}\right|\le\left(1-\frac{1140h}{3600}L\right)\left|d_{n}\right|+\frac{\left(1788+720\sqrt{5}\right)h}{3600}L\left|d_{n+u}\right|+\frac{2304h}{3600}L\left|d_{n+w}\right|+\frac{\left(1788-720\sqrt{5}\right)h}{3600}L\left|d_{n+v}\right|$$
$$-\frac{1140h}{3600}L\left|d_{n+1}\right|+\frac{25h^{5}}{336}y^{*(5)}\left(\xi_{n}\right)+R_{6}.$$

This simplifies to

$$\left(1+\frac{1140h}{3600}L\right)\left|d_{n+1}\right|\le\left(1-\frac{1140h}{3600}L\right)\left|d_{n}\right|+\frac{\left(1788+720\sqrt{5}\right)h}{3600}L\left|d_{n+u}\right|+\frac{2304h}{3600}L\left|d_{n+w}\right|$$
$$+\frac{\left(1788-720\sqrt{5}\right)h}{3600}L\left|d_{n+v}\right|+\frac{25h^{5}}{336}y^{*(5)}\left(\xi_{n}\right)+O\left(h^{6}\right)$$

As $h\to 0$ with the exception of $\left|d_{n}\right|$ every other term on the right hand side tends to zero while on the left hand side we are left with $\left|d_{n+1}\right|$ and by definition of convergence, we have

$$\lim_{h\to 0}y_{n+1}=y_{n+1}^{*}.$$

The convergence of y_{n+1} is established in agreement with the works of Ismail et al. (2020) and Akinola and Akoh (2023). Therefore, it can be shown that the other members of the block, y_{n+u}, y_{n+w} and y_{n+v} converge. Hence, we have shown that the new block hybrid numerical integrators are convergent, the remainder term R_6 which is defined as

$$R_{p+2}=C_{p+2}h^{p+2}y^{*(p+2)}\left(\xi\right)=O\left(h^{6}\right).$$

Therefore, the highest order of convergence of the new block hybrid methods is 6.

3.4 Regions of Absolute Stability of the Hybrid Methods

It is a combination of order and stability which ensures convergence of a numerical scheme to the exact solution. Here we choose to utilize the capabilities of our computer algebra system to automate the task of finding stability regions for numerical methods in the following section of the paper.

The concept of linear stability or stability is very important in the study of newly derived method, where it is used to determine the long-term behavior of a system and to identify critical points that determine the stability of the system. It is also used in control theory to design controllers that stabilize unstable systems, and in engineering and physics to study the stability of structures and fluid flows. The step-length $\Delta x\to 0$ characterizes the behavior of the underlying numerical technique. This behavior is connected to the idea of zero stability, which we discussed earlier in subsection 3.2 and is related to the behavior of the method. In other situations, though, a practical point of view requires a different idea of stability. To be stable, a numerical method must be able to reliably give results for some non-zero value of the step-length, denoted here by the notation $h>0$. For the numerical approach that is being considered, this kind of behavior is referred to as the linear stability behavior, and it involves applying the strategy described by Dahlquist (1963) for solving a linear test problem of the form

$$\frac{dy(t)}{dt} = \lambda y(t), \quad \lambda \in \mathbb{C} \text{ and } \Re\lambda < 0, \ (\mathbb{C} \text{ is a complex number}), \tag{20}$$

with a fixed positive step size $h > 0$ is usually used since it is very helpful in predicting the stability behavior of numerical methods. In such a typical stability analysis for (20) which is considered as having oscillatory solution, any of either, $A(\alpha)$*-stable, A-stability, L-stability* is very much preferred. It is an established fact that $R(z)$ the stability function is a major tool to measure the stability behavior of numerical solution. But, since our numerical integration methods are first aimed for numerical solution of singularly perturbed or dynamical systems (using block hybrid collocation methods) we suppose that the methods should possess unlimited regions, that is, *A-stability*. Note, that in particular the *A-stability* and *L-stability* properties were originally introduced as criteria which show how well numerical approximations trace the important properties of the exact solutions in form of the exponential function. Therefore, to study the stability properties of the block hybrid collocation methods we reformulate (11) and (12) as general linear methods (see, Burrage and Butcher (1979, 1980). Hence, we use the notations introduced by Butcher (2008) where a general linear method is represented by the partitioned $(s+r)\times(s+r)$ matrices (containing A, U, B and V). For the sake of simplicity, we swap the matrices U, V with C, D, respectively. These matrices are denoted in a simplified form as

$$A = (a_{ij})s,s, \quad C = (c_{ij})s,r, \quad B = (b_{ij})r,s, \quad D = (d_{ij})r,r. \tag{21}$$

The formulae for the stage values and the output values using Kronecker product notations for an N-dimension problem, gives

$$\begin{aligned} Y &= e \otimes y_n + h(A \otimes I_N)F(Y), \\ y_{n+1} &= y_n + h(b^T \otimes I_N)F(Y), \end{aligned} \tag{22}$$

where

$$e = [1]_{s\times 1}, \quad A = \lfloor a_{ij} \rfloor_{s\times s}, \quad b = [b_i]_{s\times 1}$$

and

$$Y = \begin{bmatrix} Y_1 \\ Y_2 \\ \vdots \\ Y_s \end{bmatrix}, \qquad F(Y) = \begin{bmatrix} f(Y_1) \\ f(Y_2) \\ \vdots \\ f(Y_s) \end{bmatrix}. \tag{23}$$

The coefficients of, A, C, B and D show the relationship between the numerical quantities which arise in the determination of the region of absolute stability (RAS).
For the stability regions, we adopt the approach of Akinola and Akoh (2023) where the block hybrid numerical integrators are expressed as:

$$\begin{pmatrix} a_{11} & \cdots & a_{1n} \\ \vdots & \ddots & \vdots \\ a_{n1} & \cdots & a_{nn} \end{pmatrix}\begin{pmatrix} y_{n+u} \\ \vdots \\ y_{n+1} \end{pmatrix} = \begin{pmatrix} b_{11} & \cdots & b_{1n} \\ \vdots & \ddots & \vdots \\ b_{n1} & \cdots & b_{nn} \end{pmatrix}\begin{pmatrix} y_{n-u} \\ \vdots \\ y_{n} \end{pmatrix} +$$

$$\begin{pmatrix} c_{11} & \cdots & c_{1n} \\ \vdots & \ddots & \vdots \\ c_{n1} & \cdots & c_{nn} \end{pmatrix}\begin{pmatrix} f_{n+u} \\ \vdots \\ f_{n+1} \end{pmatrix} + \begin{pmatrix} d_{11} & \cdots & d_{1n} \\ \vdots & \ddots & \vdots \\ d_{n1} & \cdots & d_{nn} \end{pmatrix}\begin{pmatrix} f_{n-u} \\ \vdots \\ f_{n} \end{pmatrix}$$

with

$$AY_m = BY_{m-1} + hCF_m + hDF_{m-1}. \tag{24}$$

Using method (12) to show the calculation of region of absolute stability following Akinola and Akoh (2023) we have the method expressed as

$$A = \begin{bmatrix} 1 & 0 & 0 & 0 \\ 0 & 1 & 0 & 0 \\ 0 & 0 & 1 & 0 \\ 0 & 0 & 0 & 1 \end{bmatrix}\begin{bmatrix} y_{n+u} \\ y_{n+w} \\ y_{n+v} \\ y_{n+1} \end{bmatrix}, \qquad B = \begin{bmatrix} 0 & 0 & 0 & 1 \\ 0 & 0 & 0 & 1 \\ 0 & 0 & 0 & 1 \\ 0 & 0 & 0 & 1 \end{bmatrix}\begin{bmatrix} y_{n-u} \\ y_{n-w} \\ y_{n-v} \\ y_{n} \end{bmatrix},$$

$$C = \begin{bmatrix} \frac{1974-870\sqrt{5}}{3600} & \frac{24192-11520\sqrt{5}}{3600} & \frac{9174-4110\sqrt{5}}{3600} & \frac{-12270+5550\sqrt{5}}{3600} \\ \frac{464+270\sqrt{5}}{9600} & -\frac{2688}{9600} & \frac{464-270\sqrt{5}}{9600} & \frac{1030}{9600} \\ \frac{9174+4110\sqrt{5}}{3600} & \frac{24192+11520\sqrt{5}}{3600} & \frac{1974+870\sqrt{5}}{3600} & \frac{-12270-5550\sqrt{5}}{3600} \\ \frac{1788+720\sqrt{5}}{3600} & \frac{2304}{3600} & \frac{1788-720\sqrt{5}}{3600} & \frac{-1440}{3600} \end{bmatrix}\begin{bmatrix} f_{n+u} \\ f_{n+w} \\ f_{n+v} \\ f_{n+1} \end{bmatrix},$$

$$D = \begin{bmatrix} 0 & 0 & 0 & \frac{2127+9150\sqrt{5}}{3600} \\ 0 & 0 & 0 & \frac{5530}{9600} \\ 0 & 0 & 0 & \frac{21270-9150\sqrt{5}}{3600} \\ 0 & 0 & 0 & \frac{1140}{3600} \end{bmatrix}\begin{bmatrix} f_{n-u} \\ f_{n-w} \\ f_{n-v} \\ f_{n} \end{bmatrix}.$$

Substituting the matrices into the characteristics equation we have

$y^{[n-1]} = M(z)y^{[n]}$, **n=1,2,…,N-1,** $z = \lambda h$,

where the stability matrix $M(z)$ is defined by

$$M(z) = D + zB(1 - zA)^{-1}C.$$

We also define the stability polynomial $\rho(\eta, z)$ by the relation

$$\begin{aligned} \rho(\eta, z) &= \det\left(\eta I - M(z)\right) \\ &= \det(r(A - Cz - DIz) - B). \end{aligned} \tag{25}$$

The region of absolute stability of the method $\Re$ is given by

$$\Re = x \in C : \rho(\eta, z) = 1 \Rightarrow |\eta| \le 1.$$

These are plotted to produce the required graphs of the regions of absolute stability of the hybrid collocation methods as shown in Figure 1.

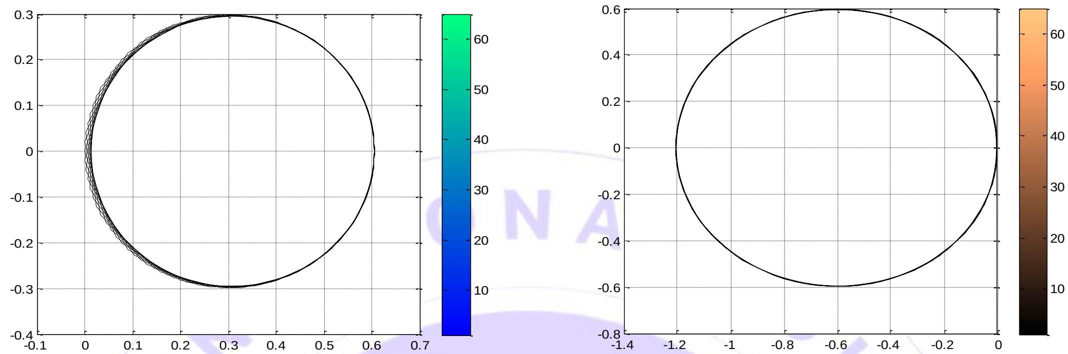

Method(11) Method(12)

(i) Regions of Absolute Stability of the newly constructed methods using ordinary plots

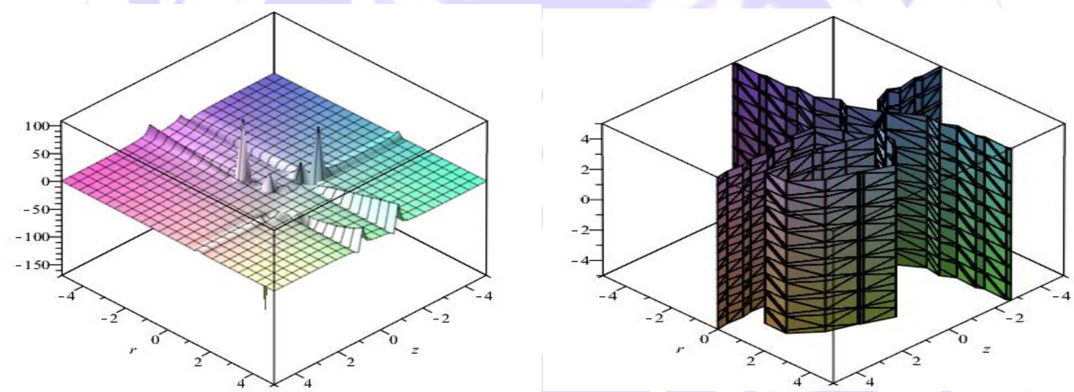

(ii) The graphic surface for method (11) using 3D and log mode implicit plots

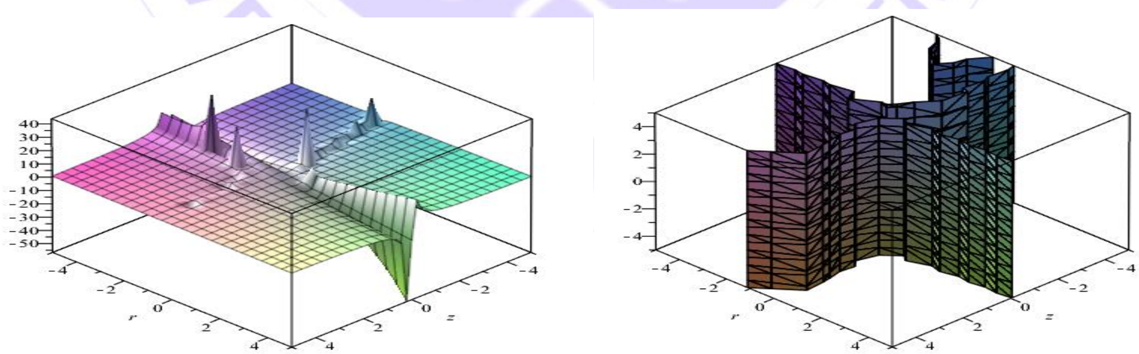

(iii) The graphic surface for method (12) using 3D and log mode implicit plots

Figure 1: *Regions of absolute stability of the hybrid methods with graphic surfaces* ***3D-(D****-Dimension)*

Remark: *The stability of the proposed methods given in (11) and (12) where as their absolute stability regions are plotted in Figure 1(i) that contains the complex plane. The corresponding 3D graphics surfaces (3D stability surfaces) for the proposed third-and fourth-order methods are also shown in Figure1 (ii) and (iii), respectively. For a method having a nonlinear structure, considerations concerning regions of absolute stability are an old concept. Nowadays, the concept has been taken over by the new concept of graphic surface of a nonlinear function. Some of the renowned works (see, Qureshi et al. (2021) and Ramos et al. (2021) introduced theoretical aspects of the graphic surface that are now considered to be the most powerful approach for the formulation and analysis of numerical schemes.*

4. Results and Discussion

In this research work, an attempt is made to devise a family of methods which has been found to be stable. This feature makes them more suitable for solving stiff and singularly perturbed systems in ordinary differential equations. These methods have demonstrated their ability to handle different type of problems with different difficulties in solving them numerically. We apply the newly derived methods to stiff, singular, and singularly perturbed initial value problems (IVPs), each with its peculiarity. Here, we use a fixed step size to show their capability in handling the mentioned problems, some of which have singularities and cannot be solve with method of limited region of absolute stability. We use Matlab codes to implement the new derived methods. In the discussion of results we use nfe to represent number of function evaluations and Ext to stand for the exact solutions for comparison purposes.

Example 1: A singularly perturbed IVP (see, Ramos et al. (2010)): In the following a nonlinear singularly perturbed initial value problem which is a pseudo-second-order kinetic equation used to describe time evolution of adsorption under non equilibrium is considered in the interval [0, 1],

$$\begin{cases} \varepsilon u'(x) = u(x) - u(x)^3, & x \in [0,1], \\ u(0) = 0.1, \end{cases}$$

with the exact solution given as,

$$u(x) = \frac{\exp\left(\frac{x}{\varepsilon}\right)}{\sqrt{99 + \exp\left(\frac{2x}{\varepsilon}\right)}}$$

The maximum point wise error obtained from the solution on uniform mesh are given in Table 2 which shows that the hybrid algorithm is working for the given value of the parameter $\varepsilon = 10^{-2}$ on the uniform mesh. As observed the new method performed better than the method in Yakubu et. al. (2023). Thus, the two methods were obtained from polynomial nodes.

Table 2: Absolute errors in the numerical integration of Example 1

x	u	Method (11) $\lvert u(t) - u_n(t) \rvert$	Yakubu et al.(2023) $\lvert u(t) - u_n(t) \rvert$
2	u	**1.053492207543638 × 10^{-05}**	**4.096607446246153 × 10^{-03}**
50	u	**6.280533093594443 × 10^{-09}**	**1.462301231214269 × 10^{-07}**
150	u	**1.110223024625157 × 10^{-16}**	**1.110223024625157 × 10^{-16}**
250	u	**1.110223024625157 × 10^{-16}**	**1.110223024625157 × 10^{-16}**

500	u	**3.330669073875470 × 10^{-16}**	**3.330669073875470 × 10^{-16}**

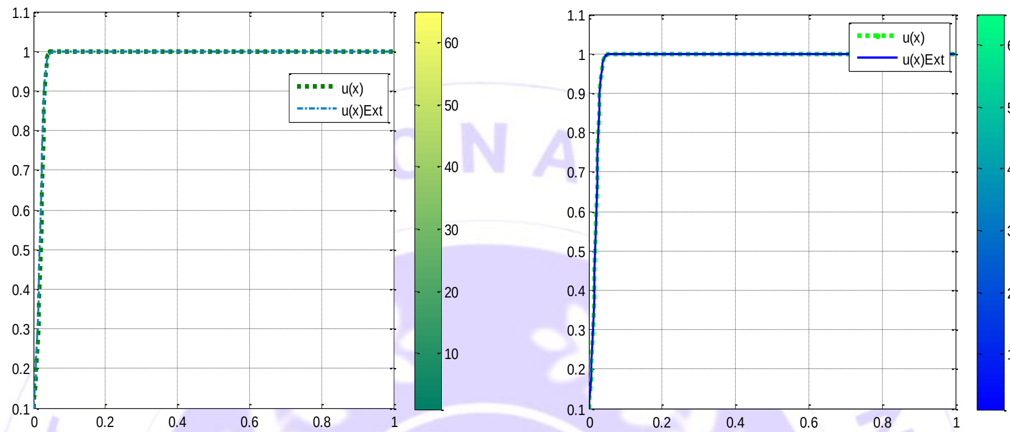

Figure 2: *Solution curves for Example 1 using the new methods with nfe =500*

Example 2: A nonlinear Riccati equation: This problem is coupled with initial value given by

$$u'(x) = -4 + 4u(x) - u(x)^2, \qquad u(0) = 1,$$

whose exact solution is $u(x) = 2x - 1/x - 1$ and also has a pole at $x = 1$. This is a very challenging singular nonlinear problem, especially for method with limited region of absolute stability. Based on the solutions presented below, the two methods have no difficulty in dealing with problem of this type. We observed that the bigger the number of steps is so is the corresponding error. The solution curves are shown in Figure 3a and 3b, while graphic surface curves are displayed in 3c and 3d respectively.

Table 3: Absolute errors in the numerical integration of Example 2

x	u	Yakubu et al.(2004) $\lvert u(t) - u_n(t) \rvert$	Method(12) $\lvert u(t) - u_n(t) \rvert$
2	u	**2.684297228938704 × 10^{-12}**	**8.038014698286133 × 10^{-14}**
50	u	**1.354034662170989 × 10^{-10}**	**3.935629599993717 × 10^{-12}**
150	u	**4.377839202263090 × 10^{-10}**	**1.196909238387889 × 10^{-11}**
250	u	**7.788761857696613 × 10^{-10}**	**2.000277721236898 × 10^{-11}**
500	u	**1.836328311632940 × 10^{-09}**	**4.009115261993657 × 10^{-11}**

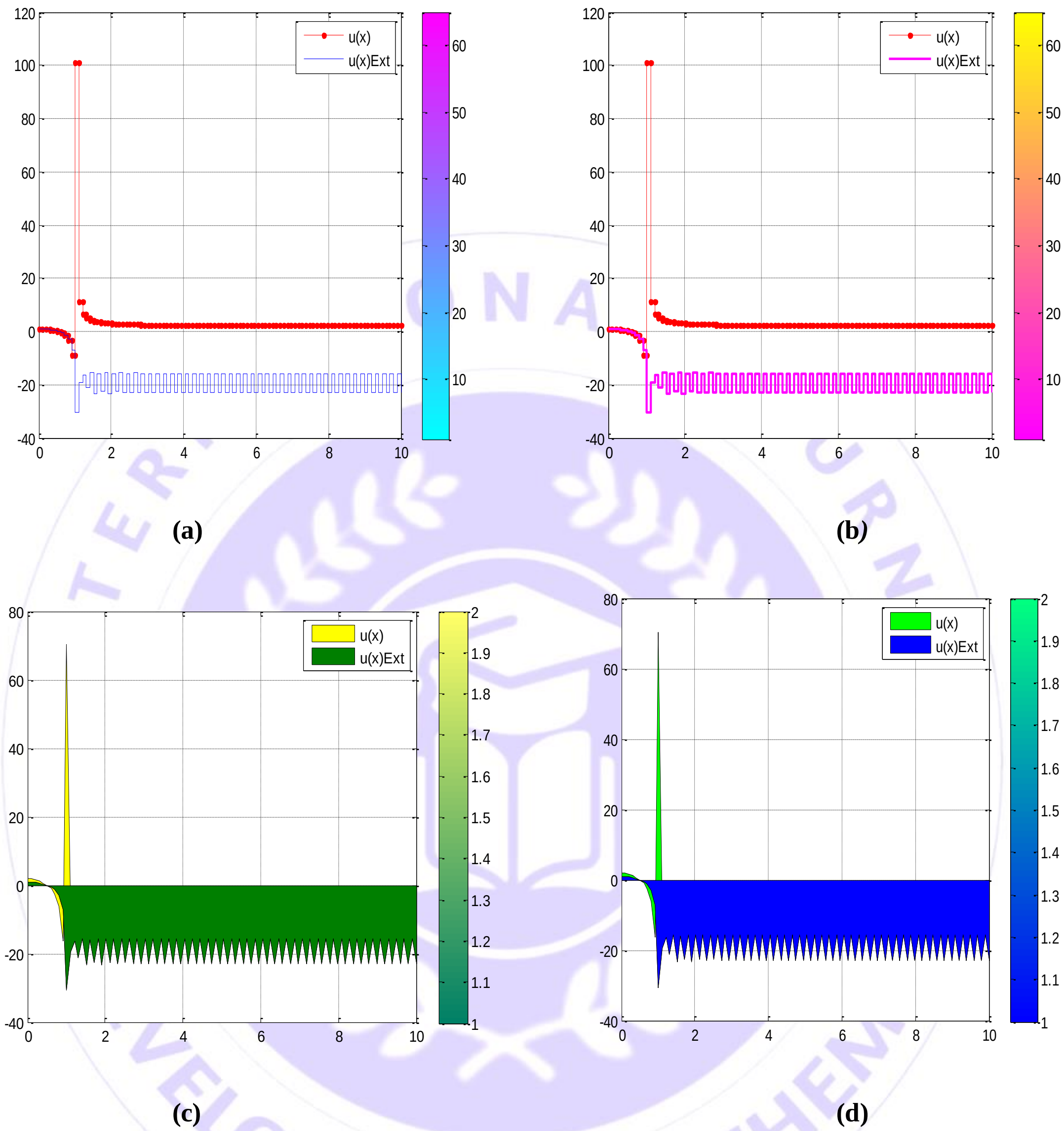

Figure 3: *Graphic surface curves for Example 2 using the new method with nfe =500*

Example 3: A singularly perturbed IVP Ramos et al. (2010): This problem is characterized by the presence of a small perturbation parameter ε in the solution or discontinuity. The problem is given by

$$\begin{cases} \varepsilon u'(x) = \exp(-u), & x \in [0,1], \\ u(0) = 0, \end{cases}$$

whose exact solution is given as,

$$u(x) = \log\left(1 + \frac{x}{\varepsilon}\right)$$

Upon the application of the derived new methods for the small parameter $\varepsilon = 10^{-2}$ the maximum pointwise absolute errors on the nodal points in the integration interval are obtained as shown on the Table of values below, which indicates the necessity of the uniform order method for singularly perturbed initial value problems. As observed, one can see the third order convergence from these results.

Table 4: Absolute errors in the numerical integration of Example 3

x	u	Method (11) $\lvert u(t) - u_n(t) \rvert$	Method (12) $\lvert u(t) - u_n(t) \rvert$
2	u	**1.338011398725747 × 10^{-09}**	**4.017898420859123 × 10^{-10}**
50	u	**5.457658576457636 × 10^{-08}**	**1.965931872220487 × 10^{-09}**
150	u	**1.186757261906202 × 10^{-07}**	**5.960124983524565 × 10^{-08}**
250	u	**1.488292379336897 × 10^{-07}**	**9.930420074612256 × 10^{-08}**
500	u	**1.675240302034808 × 10^{-07}**	**1.975274433758251 × 10^{-07}**

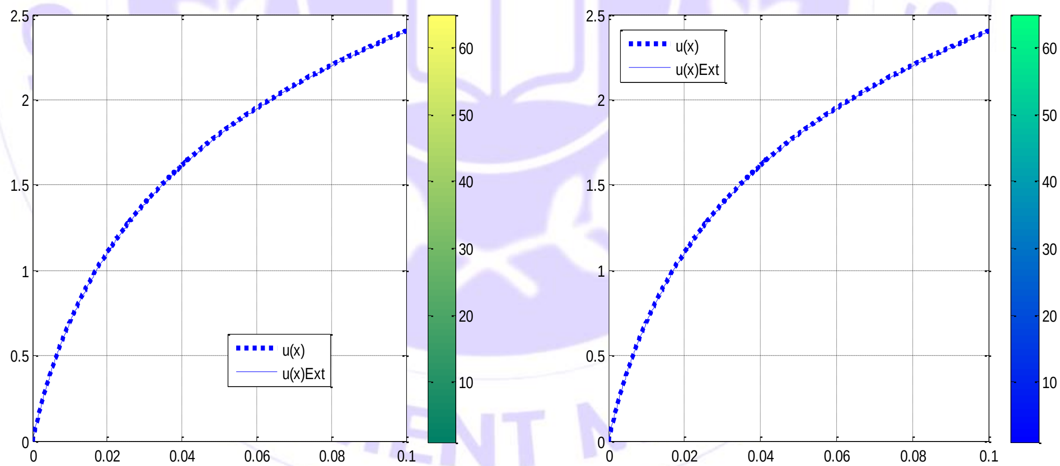

Figure 4: *Solution curves for Example 3 using the new methods with nfe =500*

Example 4: A singular initial value problem Odekunle et al. (2004) This problem is characterized by the presence of a pole in the solution or discontinuity. This problem has been used as a numerical test for different integrators intended for numerically solving singular initial value problems. The problem is given by

$$u'(x) = 1 + u(x)^2, \qquad u(0) = 1,$$

with theoretical solution $u(x) = (x + \pi/4)$ which has a simple pole when x is equal to $\pi/4$. The solution of the problem becomes unbounded in the neighbourhood of the singularity at $x = \pi/4$, as observed by Odekunle *et al*.(2004) As the right-hand side of the differential equation is a polynomial in u of second degree, our method integrates the problem exactly, that is, without local truncation error. In Table 5 we present the results obtained from the newly developed scheme which are more accurate than that obtained by Odekunle *et.al.* (2004), using an inverse Runge-Kutta scheme of order four. The obtained results are clearly better for this problem and we observe the ability of the method to overpass the singularity. In Figure 5 the exact and the discrete solution with $h = 0.1$ are shown on the interval [0, 1]. In addition, if one extends the interval of integration including more singular points, it seems that the numerical approximation follows the analytical solution without serious effects as shown in Figure 5(a, b). In the Figure we have plotted the graphic surface of both the exact and discrete solution obtained with $h = 0.1$.

Table 5: Absolute errors in the numerical integration of Example 4

x	u	Kwami *et al*. (2016) $\lvert u(t) - u_n(t)\rvert$	Method(12) $\lvert u(t) - u_n(t)\rvert$
2	u	**1.110223024625157 × 10^{-16}**	**1.110223024625157 × 10^{-16}**
50	u	**5.415745629733237 × 10^{-10}**	**5.278000259067994 × 10^{-13}**
150	u	**1.752904932317279 × 10^{-09}**	**1.612487920965577 × 10^{-12}**
250	u	**3.125618874832981 × 10^{-09}**	**2.712052804554332 × 10^{-12}**
500	u	**7.450735584058066 × 10^{-09}**	**5.519584789226428 × 10^{-12}**

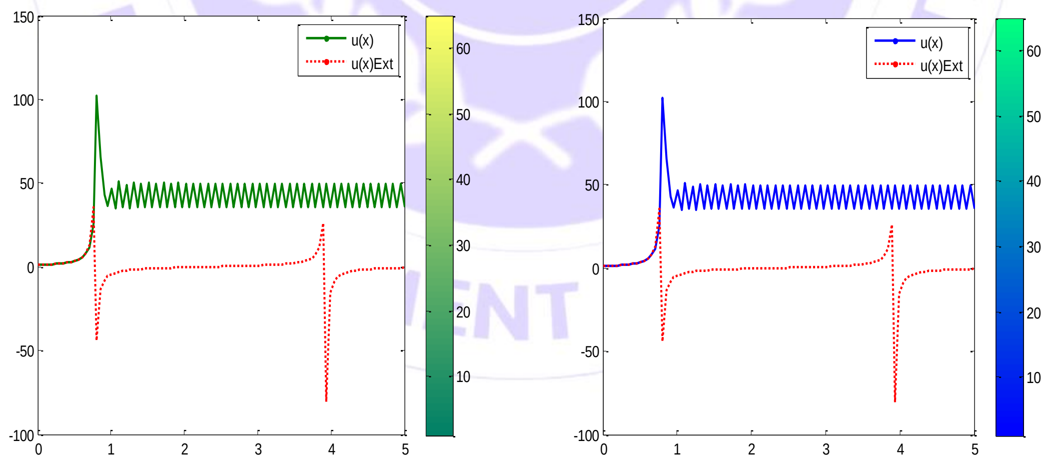

(a) (b)

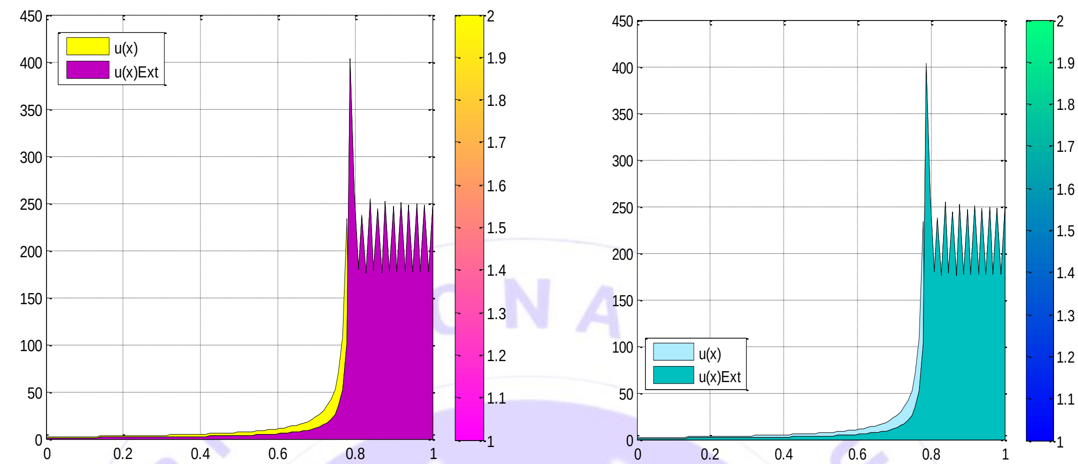

(c) (d)

Figure 5: *Graphic surface curves for Example 4 with nfe =500*

Example 5: Stiff differential equation: A stiff differential equation which involves rapidly increasing or decaying transient solution, which results in a difficulty for most of the numerical methods especially those with limited regions of absolute stability is considered. The method in (12) was tested on the problem written as

$$\begin{cases} u'(x) = -100u(x) + 99\exp(2x), & x \in [0,10], \\ u(0) = 0, \end{cases}$$

with exact solution given by,

$$u(x) = \frac{33}{34}\left(e^{2x} - e^{-100x}\right)$$

The problem has been integrated on the interval [0, 10] with h =0.1 and the results are presented in Table 6, while the graphic surface plots are shown in Figure 6.

Table 6: Absolute errors in the numerical integration of Example 5

x	u	Method (12) $\lvert u(t)-u_n(t)\rvert$	Kwami et al.(2016) $\lvert u(t)-u_n(t)\rvert$
2	u	**3.339342691255354 × 10^{-17}**	**4.943961906533900 × 10^{-17}**
50	u	**5.551115123125783 × 10^{-17}**	**6.800116025829084 × 10^{-16}**
150	u	**1.110223024625157 × 10^{-16}**	**2.053912595556540 × 10^{-15}**
250	u	**2.775557561562891 × 10^{-16}**	**2.331468351712829 × 10^{-15}**
500	u	**1.110223024625157 × 10^{-16}**	**3.330669073875470 × 10^{-15}**

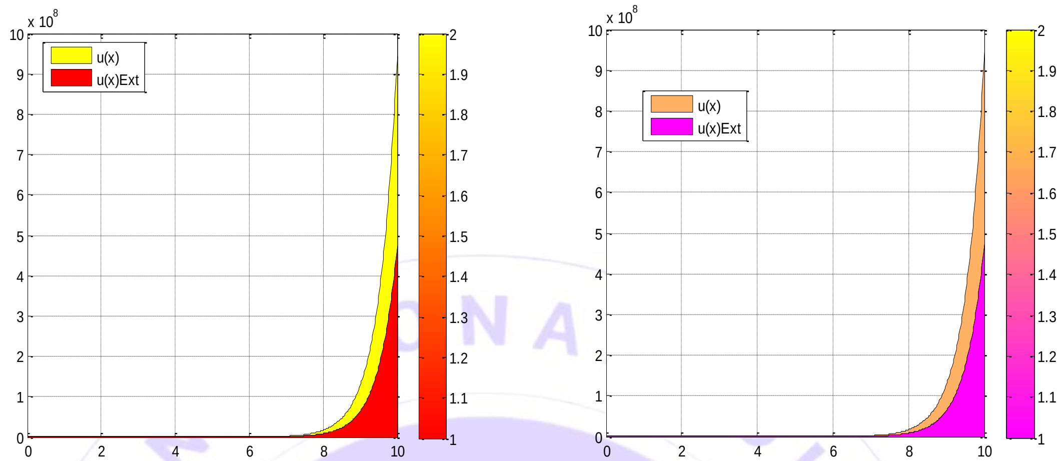

Figure 6: *Graphic surface curves for Example 5 with nfe =500*

5. Conclusion

In this study, we have formulated two numerical methods for approximating both linear and nonlinear singularly perturbed initial value problem in ordinary differential equations. This was accomplished through the combination of various collocation techniques. Specifically, we employed a one-step and multistep collocation processes to develop the hybrid collocation methods of third and fourth orders. Our analysis indicates that these methods exhibit convergence when appropriate stability and consistency conditions are fulfilled. In conclusion, we support our analysis with several test problems and computationally validate the convergence order of the methods, as illustrated in the accompanying Table of values and the efficiency graphic surface curves presented in the previous section's Figures. In a forthcoming publication, we will discuss implicit block hybrid collocation methods capable of achieving high orders, including symmetry characterization. Additionally, we aim to broaden the applications of block hybrid collocation methods to address modeled differential equations encountered in various fields, including cardiac electrophysiology and tumor-immune interaction population models.

Acknowledgements: The authors are grateful to the anonymous reviewers and the handling editor for their constructive observations and suggestions which enhanced the manuscript.

Conflict of interest: The authors declare that, there is no conflict of interest for the study.

References

Akinola, R. O., Akoh, A.S. (2023). A seventh-order computational algorithm for the solution of stiff systems of differential equations, *J. Nig. Math. Soc.* **42**(3), 215 – 242.

Aris, R. (1969). On stability criteria of chemical reaction engineering. *Chem. Eng. Sci*. **24,** 149 - 169.

Burghardt, A., Zaleski, T.(1968), Longitudinal dispersion at small and large Peclet numbers in chemical flow reactors, *Chem. Eng. Sci.* **23,** 575–591.

Burrage, K., Butcher, J.C.(1979). Stability criteria for implicit Runge-Kutta method, *SIAM J. Numer. Anal.,* **16**, 46 – 57.

Burrage, K., Butcher, J. C. (1980). Nonlinear stability for a general class of differential equations, *BIT, Numer. Math.*, **20**, 185 **-** 203.

Butcher, J. C. (1987). The Numerical Analysis Of Ordinary Differential Equations: Runge-Kutta and General Linear Methods. John Wiley and Sons, Ltd.

Butcher, J. C. (2003). Numerical methods for ordinary differential equations, John Wiley & Sons Ltd.

Butcher, J. C. (2008). Numerical Methods for Ordinary Differential Equations, Second Edition, John Wiley & Sons, Ltd.

Dahlquist, G. (1963). A special stability problem for linear multistep methods, *BIT J. Numer. Math.*, **3**, 27 – 43.

Fatunla, S. O. (1991). Block methods for second order ODEs, *Intern. J. Comput. Math.,* **41**, 55–63.

Higinio Ramos, Vigo-Aguiar, J., Natesan, S., García-Rubio, R., Queiruga, M. A. (2010). Numerical solution of nonlinear singularly perturbed problems on nonuniform meshes by using a non-standard algorithm, *J. Math. Chem.*, **48,** 38–54.

Ismail, N. I. N, Majid, Z. A., Senu, N. (2020). Solving neutral delay differential equation ofpantograph type, *Malaysian Journal of Mathematical Sciences* 14(S) 107-121.

Kwami, A. M., Kumleng, G.M., Kolo, A. M., Yakubu, D.G. (2016). Block hybrid multistep methods for the numerical integration of stiff systems of ordinary differential equations arising from chemical reactions, *Abacus, J. Math. Asso. Nig.* **42**(2) 134 – 164.

Lambert, J. D. (1973). *Computational Methods in Ordinary Differential Equations*, John Willey and Sons. New York.

Lambert, J. D. (1991). *Numerical Methods for Ordinary Differential Systems. The Initial Value Problem*, John Willey and Sons. New York.

Odekunle, M.R., Oye, N.D., Adee, S.O. (2004). Ademiluyi, R. A., A class of inverse Runge–Kutta schemes for the numerical integration of singular problems, *Appl. Math. Comput.* **158**, 149–158.

Qureshi, S., Soomro, A., Evren Hıncal, E. (2021). A new family of A- acceptable nonlinear methods with fixed and variable step-size approach, *Compt. Math. Meth.* **3**(6) e1213.

Ramos, H., Patricio, M. F. (2014). Some new implicit two-step multi-derivative methods for solving special second-order IVP's, *Appl. Math. Comp.,* **239**, 227- 241.

Ramos, H., Qureshi, S., Soomro, A. (2021), Adaptive step size approach for Simpson'-type block methods with time efficiency and order stars, *Compt. Appl. Math.*,**40,** 219.

Yakubu, D. G., Onumanyi, P., Chollom, J. P. (2004). A new family of general linear methods based on the block Adams-Moulton multistep methods. *J. of Pure and Applied Sciences,* **7** (1) 98 -106.

Yakubu, D. G., Kumleng, G. M., Markus, S. (2017). Second derivative Runge-Kutta collocation methods based on Lobbatto nodes for stiff systems, *J. Mod. Meth. Numer. Math*., **8**(1-2)118-138.

Yakubu, D. G., Mohammed, A. Tahiru, A.G., Abubakar, K. S., Adamu, M. Y. (2023). Numerical simulation of nonlinear dynamics of breast cancer models using continuous block implicit hybrid methods, *Fractal and Fractional* **7**(3), 237.